



# READ 2024

RESEARCH & EDUCATION IN AIRCRAFT DESIGN  
WARSAW, POLAND | 6-8 NOVEMBER 2024



## KINEMATIC SIMULATION IN THE AIRCRAFT LANDING GEAR DESIGN AND OPTIMIZATION PROCESS

Jakub Suszyński<sup>1</sup>, Mariusz Kowalski<sup>2</sup>, Tomasz Antoniewski<sup>3</sup>

<sup>1</sup>Warsaw University of Technology

<sup>2</sup>Aircraft Design Division, Warsaw University of Technology

<sup>3</sup>AT-P Aviation Sp.z.o.o.

### Abstract

The paper focuses on supporting the mechanical design process of the landing gear for a general aviation aircraft using available simulation modules and CAD/CAM/CAE software. The article is based on the analysis, modification, and optimization of the landing gear system of the AT-5 aircraft. A wide range of kinematic simulations and structural analyses were conducted using NX Motion and NX Nastran software, with a specific focus on the landing gear's retraction and deployment mechanisms. These analyses were carried out under conditions outlined by CS-23 regulations. Through these simulations, the study enabled identification of the loads acting on the landing gear extension system during various operational phases. The results enabled the selection of appropriate actuators and the determination of the necessary strength for key components and connections.

Following the initial design phase, modifications were introduced to optimize the system further. These modifications aimed not only at improving functionality but also at reducing the overall weight of the landing gear. This approach exemplifies the power of simulation-driven engineering in advancing modern mechanical design practices, delivering tangible benefits that extend well beyond the scope of the project.

**Keywords:** structure, fea, kinematics, optimisation, landing gear

### 1. Introduction

The landing gear system is a vital structural component of an aircraft, designed to support the full weight of the aircraft during ground operations, including taxiing, take-off, and landing. It ensures stability and absorbs the impact loads during touchdown, playing a critical role in the overall safety and performance of the aircraft. [1]

With evolving technological advancements, the use of kinematic simulations in the design and optimization of landing gear systems has become indispensable. Modern landing gear systems have become complicated so that preparing the analytical model may be highly demanding.

This paper focuses on the application of kinematic simulation in the design and optimization process of aircraft landing gear, utilizing Siemens NX Motion software. Kinematic simulation enables to visualize and analyse the movement, forces, and interactions within the landing gear system under various operating conditions. It provides insights into the mechanical behaviour, allowing for the identification of potential issues such as interference, excessive stress, or improper motion range before physical prototyping begins.

The study covers the analysis of AT-5's gear retraction/extension system. In addition to the analysis the modifications of the system were described.

### 1.1 AT-5 Aircraft

The AT-5 is a three-seat, low-wing metal aircraft designed for both training and tourism purposes. Its retractable tricycle landing gear system features two main legs attached to the wing structure, which retract outward toward the wingtips, and a nose gear that retracts rearward into the fuselage. The nose gear is equipped with a dampened, steerable leg that is retracted through an electric actuator system. This system also includes an emergency extension mechanism that mirrors the functionality of the main landing gear emergency extension system.



Figure 1 - AT-5 Aircraft [2]

### 2. Preparation of the computational model

The landing gear extension and retraction system consists of an electric actuator, a lever assembly, a pivot shaft, and a linkage connected to the upper breaker strut. The pivot shaft, along with the levers, can rotate around an axis defined by bearings placed in the fittings. This rotation is facilitated by transferring the motion of the actuator's end as it extends or retracts. The change in the angular position of the components causes the linkage, connected to the upper breaker strut, to move, leading to the rotation of this part around the axis defined by the upper breaker strut fitting. As a result of the lower breaker strut being attached to the landing gear leg, this operation causes the locking and unlocking of the breaker strut, which moves the entire landing gear assembly.

## KINEMATIC SIMULATION IN THE AIRCRAFT LANDING GEAR DESIGN AND OPTIMIZATION PROCESS

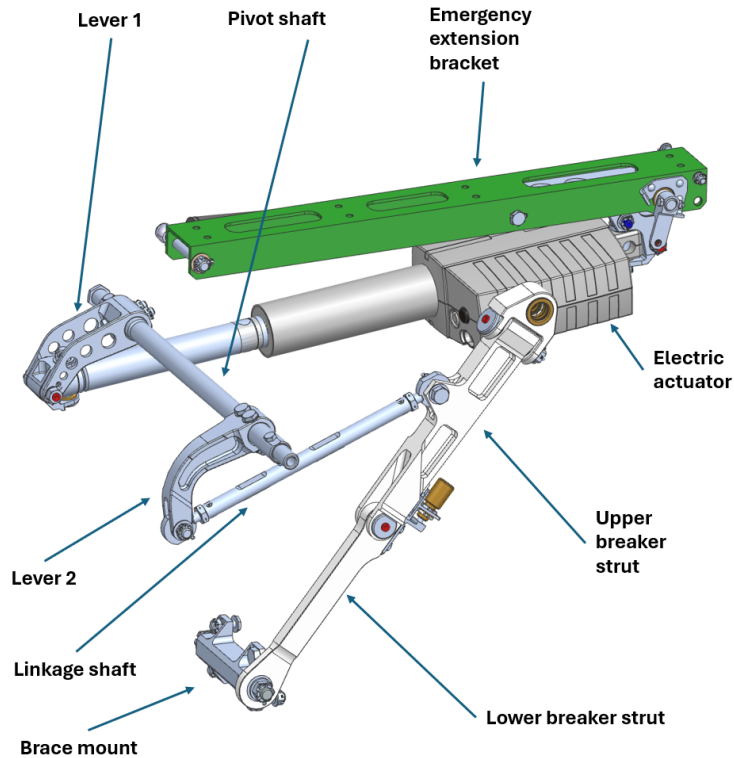


Figure 2 - AT-5 landing gear extension system

The complete 3D model of the system was prepared, stressing the need for accurate mass data. In order to reduce the complexity of the model, the substitution of the shock absorber was created.

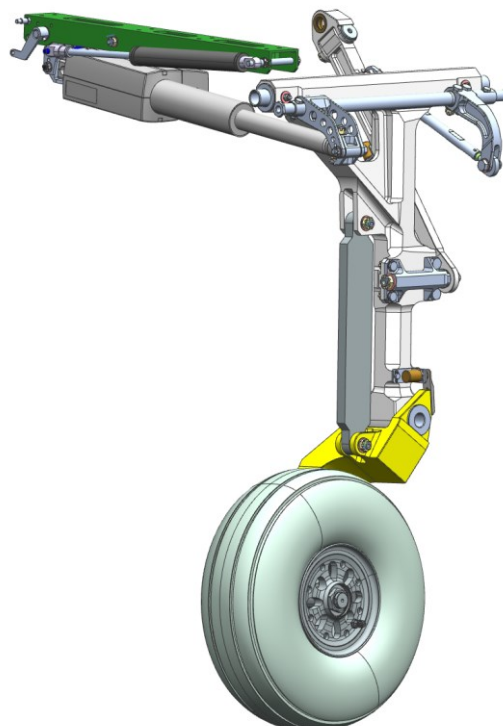


Figure 3 - Complete 3D model of the landing gear used for the analysis.

### 2.1 Load conditions

Load conditions used for the analysis were defined in compliance with the *Certification Specifications for Normal, Utility, Aerobatic and Commuter Category Aeroplanes CS-23*. As per CS 23.729(a)(1) the landing gear extension system shall be designed for maximum flight load factors with the gear

retracted and the combination of loads during retraction at any airspeed up to  $1.6 V_{s1}$  (1.6 times clean configuration stall speed) [3]. Aerodynamic loads and friction in the system were not included in the analysis. Only inertia loads were taken into account. Three cases were created:

1. Landing gear extension, load factor  $n = 2.245$
2. Landing gear extension, load factor,  $n = 2.245$
3. Landing gear retracted, load factor,  $n = 5.131$

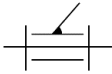



No. 1 and no. 2 are directly associated with the movement of the system. No. 3 is due to the positive load factor caused by a wind gust for retracted landing gear. The values of corresponding flight load factors were obtained from the flight loads envelope of the AT-5 aircraft.

## 2.2 Motion-body and joints creation

In order to obtain correct movement conditions of the system motion bodies and joints were created. To significantly simplify the initial analysis, it was decided to combine individual components of the chassis assembly into larger units (motion-bodies), which will be analysed as whole rigid bodies. In this case, it will not be necessary to perform calculations for each component separately, which will significantly reduce the time required for the analyses. A rule was adopted where components that do not move relative to each other are combined into one unit. Ten motion bodies were created.

To create the appropriate kinematics of the analysed system, the proper types of connections shown in Table 1. between the moving components were applied.

*Table 1 - Types of joints used in the analysis [4]*

Joint type	Constrained DOF			Schematic [5]	Comment
	Translational	Rotational	Total		
Revolute	3	2	5		Rotation around Z axis
Spherical	3	0	3		Rotation around point
Cylindrical	2	2	4		Translation along Z axis, rotation around Z axis
Slider	2	3	5		Translation along Z axis

The proper application of constraints in the analysis is extremely important as it ensures the appropriate mobility of the system. In NX Motion, when the system is over-constrained, the software automatically removes "redundant" connections. [6] In such cases, the user has no control over which constraints are removed, which may lead to incorrect results. If too few degrees of freedom are constrained, the system may also behave incorrectly.

The system mobility was determined using the Grübler-Artobolevsky formula [4]:

$$W_T = 6k - \sum_{i=1}^5 (6 - i)p_i \quad (1)$$

Where:

$k$  - The number of moving bodies, each of which has 6 degrees of freedom before being connected

$i$  - The class of a kinematic pair

$p_i$  - The number of constrained degrees of freedom

For the analysed system (prepared for dynamic analysis):

$k = 10$  (number of moving bodies),

$p_1 = 9$  (number of 1st-class pairs, revolute joints),

$p_2 = 1$  (number of 2nd-class pairs, cylindrical joints),

$p_3 = 3$  (number of 3rd-class pairs, spherical joints).

$$W_T = 6k - \sum_{i=1}^5 (6 - i)p_i = 6 \cdot 10 - (6 - 1) \cdot 9 - (6 - 2) \cdot 1 - (6 - 3) \cdot 3 = 2 \quad (2)$$

One degree of freedom is due to the unconstrained rotation of the linkage shaft. However this element is constrained geometrically via contact conditions so that  $W_T = 1$ . The obtained value indicates that the movement of the system is possible. It is not over-constrained.

For the static analysis (case no. 3) where the movement of the actuator was blocked,  $W_T = 0$ . The system is locked and the analysis can be conducted.

### 2.3 The results of the initial analysis

Based on the dynamic and static analyses of the system, the force acting on the actuator during the movement of the system has been determined. It was assumed that the tensile force on the actuator is represented by a negative sign ("-"), while the compressive force is represented by a positive sign ("+" ). Graphs of force as a function of the actuator's extension have been prepared.

Such analysis and graphical representation are crucial for the design as they provide insights into how the system will behave under different loading conditions. Determining the forces allows for selecting the appropriate actuator.

- **Case no. 1. Landing gear retraction,  $n = 2.245$**

Force during landing gear retraction,  $n=2.245$

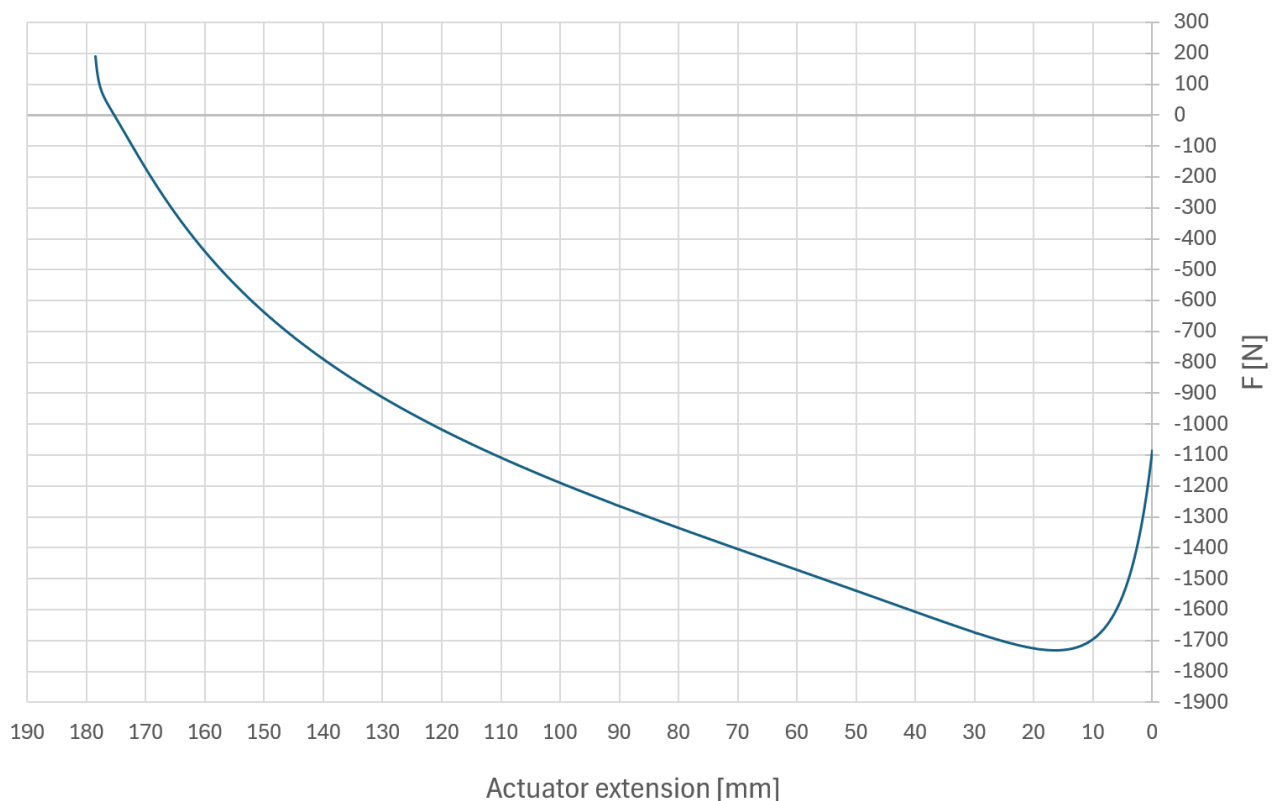


Figure 4 - Force on the actuator during LG retraction

In the initial phase of the actuator retraction, a compressive force occurs. This is due to the geometry of the system and the fact that in order to lock the landing gear in the open position, the breaker strut passes neutral point. The greatest load on the actuator occurs in the final phase of the strut retraction

when the strut is perpendicular to the direction of the gravity vector. At this point, the force acting on the actuator is  $F = -1730.979 N$ , for an actuator extension of  $s = 16.320 mm$ . After this point, the force decreases.

- **Case no. 2. Landing gear extension,  $n = 2.245$**

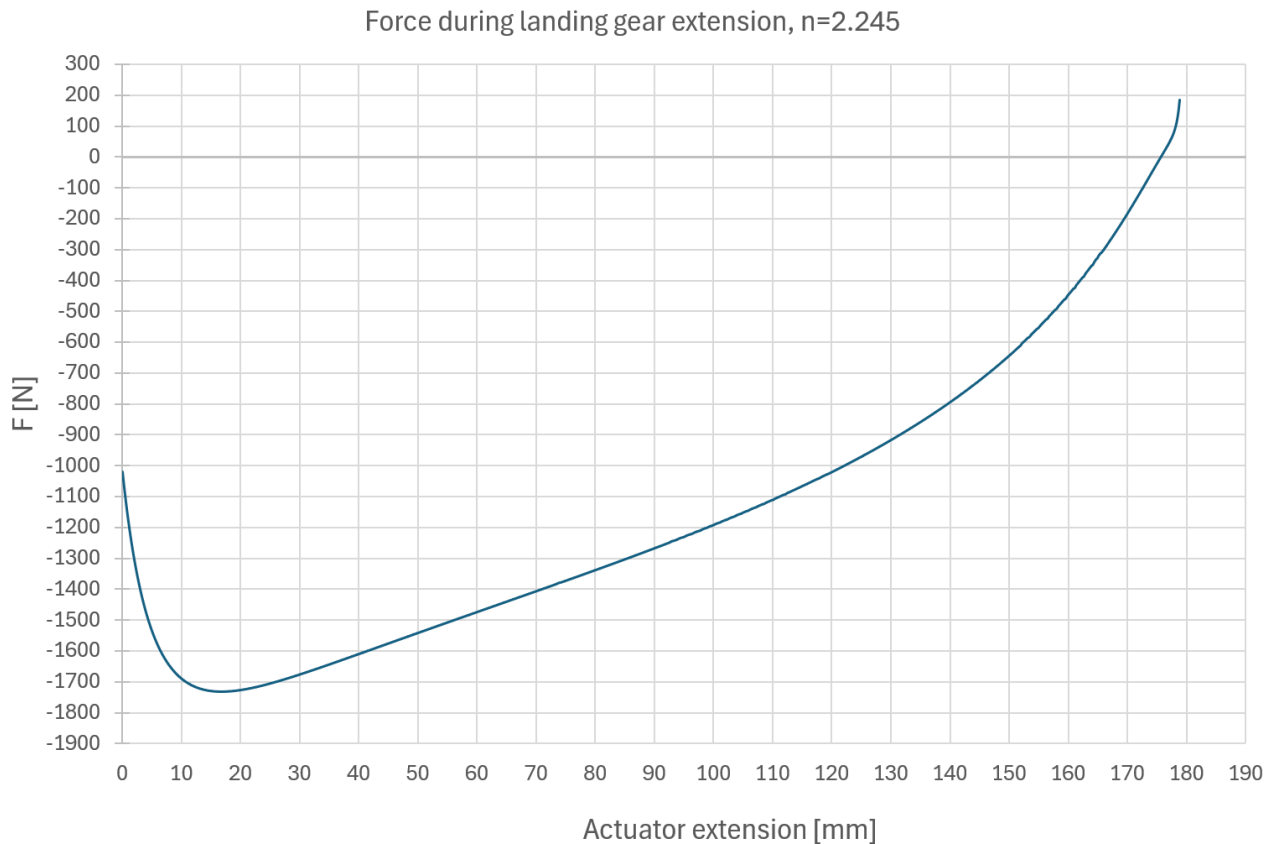


Figure 5 - Force on the actuator during LG extension

The distribution of force during the landing gear extension is almost identical to that of case 1. The maximum load on the actuator occurs in the initial phase of the movement, in a position analogous to the critical position in case 1. The tensile force at that point is  $F = -1730.979 N$

- **Case no. 3. Landing gear retracted,  $n = 5.131$**

The force acting on the actuator while the landing gear is locked in the retracted position was determined.  $F_{static} = -3809.043 N$ . It shows that the actuator shall be able to withstand the load in the retracted position.

### 3. Modification and optimisation of the system

In order to reduce the mass of the system modifications were introduced. These include changing the actuator and the geometry of the levers.

#### 3.1 Actuator selection

To find the appropriate actuator, a list of conditions that the device should meet has been prepared. These include:

- **Stroke of the actuator:**  $s=200$ , (initial assumption - no changes in geometry)
- **Maximum length of the retracted actuator:**  $l=450 mm$
- **Retraction speed under full load:**  $V=17 mm/s$
- **Working force of the actuator during extension and retraction:**  $F=2500 N$  (assumed based on conducted analyses with a margin to allow for potential changes in geometry)
- **Minimum blocking force**  $F = 4500 N$



The new actuator was selected from the offerings of leading manufacturers and meets all the specified criteria apart from required retraction speed, however a new value (12mm/s) is acceptable. The new device offers a mass reduction of 25% in comparison to the original one.

### 3.2 Changes of other elements in the system

Due to the change of the actuator, it was necessary to modify the geometry of other elements in the system. A completely new lever no. 1 was designed. Obtaining the appropriate shape and length of the component requires numerous iterations. One of the challenges in this case is the close placement of the strut, which necessitates maintaining a minimum clearance. Additionally, it is essential to determine the length of the arm in such a way that there is some allowance for the extension of the actuator, allowing for the "tightening" of the legs and the introduction of a locking force into the system. Multiple iterations were conducted. A general geometry of the lever shown in Figure 6 was prepared.

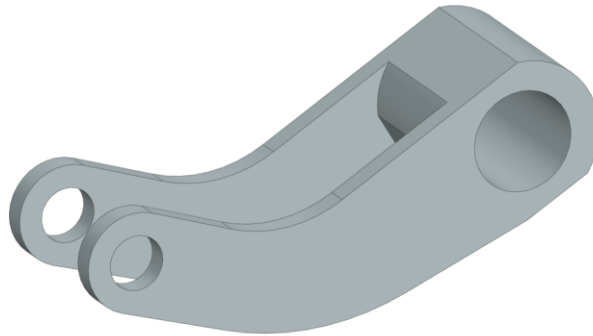


*Figure 6 - The geometry of a new lever*

### 3.3 New kinematic analysis of the system

Due to the change in the geometry of the entire system resulting from the use of a new actuator, it is necessary to re-conduct mobility analyses of the system and the forces acting during the anticipated operations. To this end, a computational model has been prepared in the NX Motion module based on the new system model shown in Figure 7.

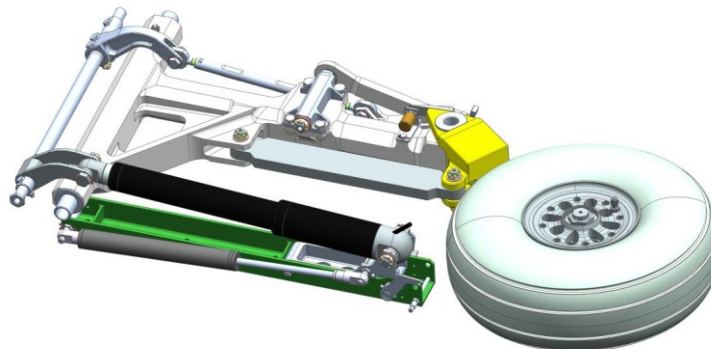


*Figure 7 - Visualization of a 3D model of the new system configuration*

Relative to the previous Motion computational model, several changes were made directly related to the alteration of the lever shape and the actuator model. Additionally, a model of the emergency landing gear release system was prepared to conduct analyses of the landing gear operations in emergency mode. This scenario was previously skipped, as it was assumed not to affect the sizing values of the actuator.

New motion bodies were created as well as new joints.  
For the new configuration there were 5 cases assumed:

1. **Landing gear retraction**,  $n=2.245$
2. **Landing gear retraction** with a constant force of 3100 N (maximum operating force of the actuator),  $n = 2.245$
3. **Landing gear extension** with a constant force of 3100 N (maximum operating force of the actuator),  $n = 2.245$
4. **Landing gear retracted and locked**,  $n = 5.131$  (vertical gust case)
5. **Emergency extension**, gas spring operating with a constant force  $F = 1000$  N

Before conducting the analysis, the Grubler coefficients had been checked and the mobility of the system had been derived. The system was constrained correctly.

### 3.4 The new analysis results

- **Case. 1. Landing gear retraction,  $n = 2.245$**

Force during landing gear retraction,  $n=2.245$

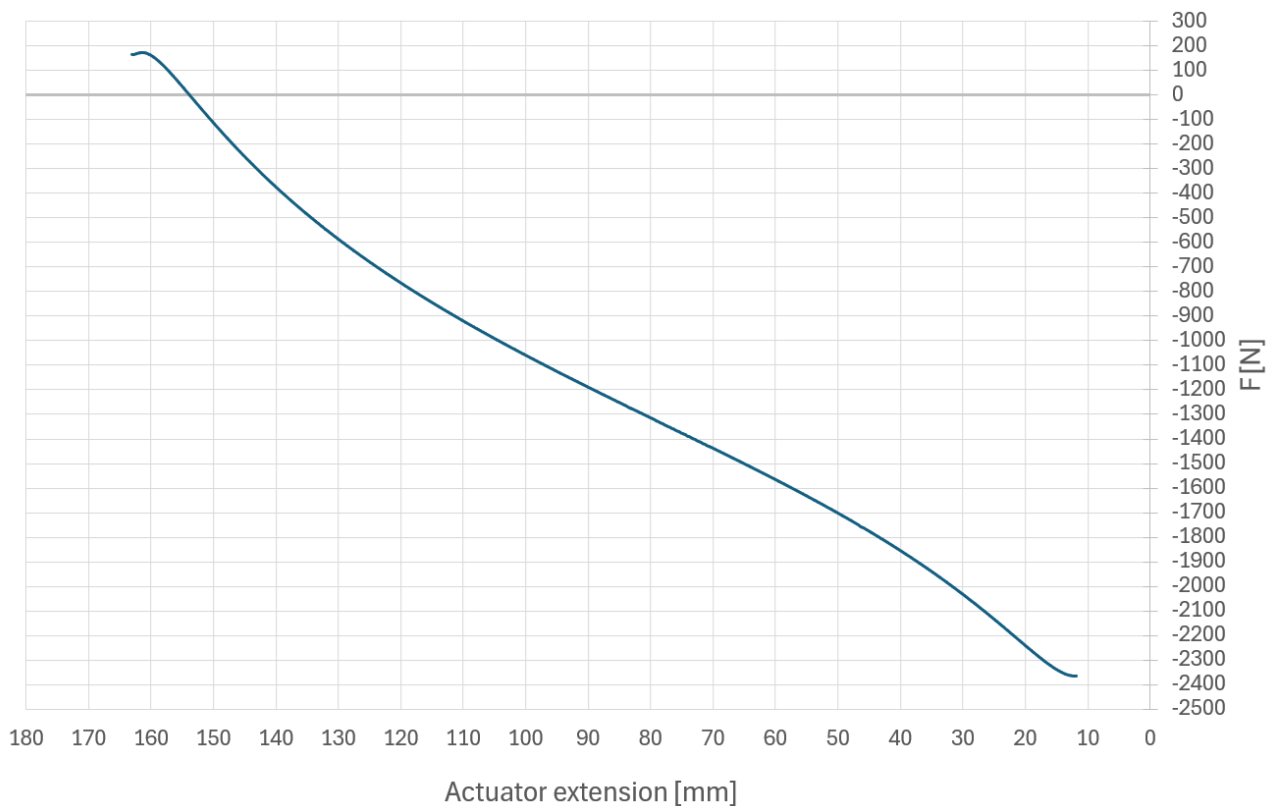


Figure 8 - Force during landing gear retraction,  $n=2.245$

The force curve has changed since the kinematic configuration changed. Maximum force has been determined:  $F = -2366.063N$ . The result shows that maximum allowable force on the actuator was not exceeded.



- **Case 2. Landing gear retraction,  $F=3100\text{N}$ ,  $n=2.245$**

The force in the joint has been analysed.

Force in the joint for max actuator force, LG retraction,  $F=3100\text{N}$ ,  $n=2.245$

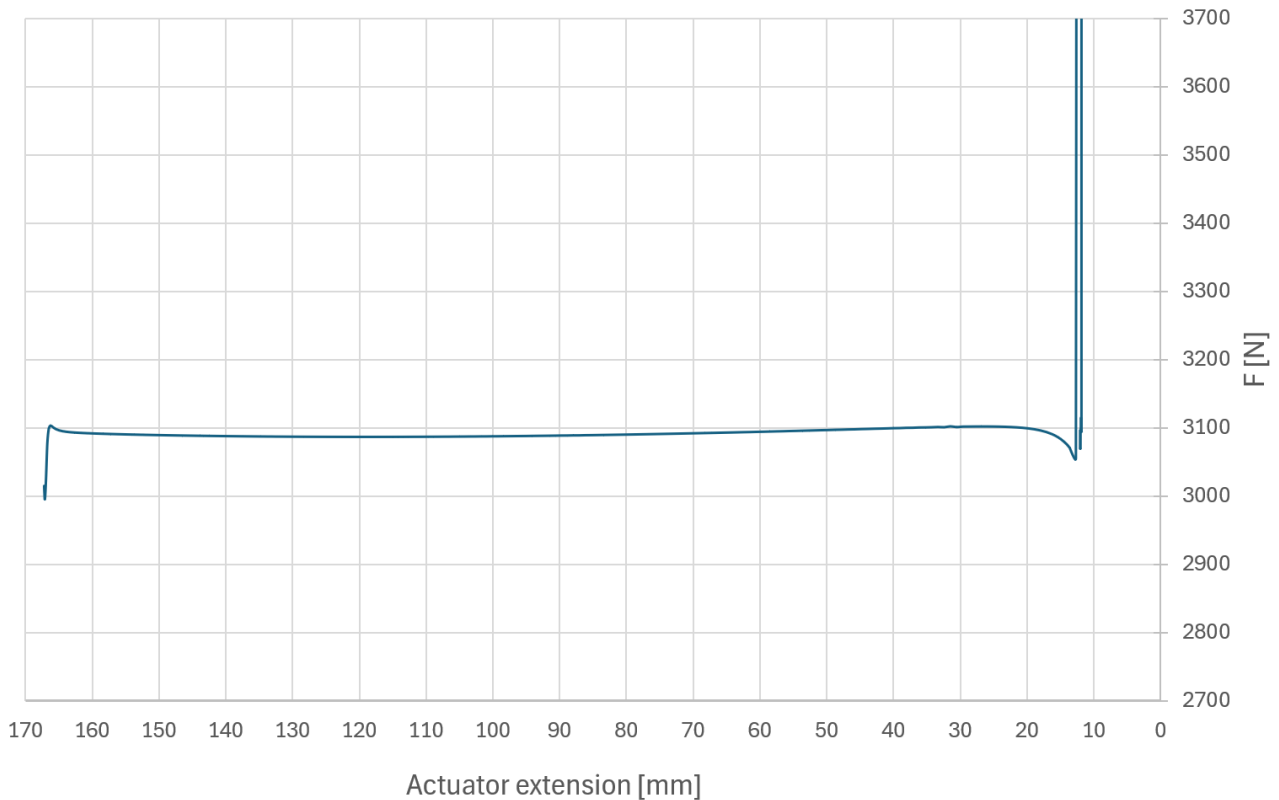


*Figure 9 - Force in the actuator joint for max actuator force*

As expected, the resultant force value is almost constant. At the beginning of the movement, there is a slight decrease in this value due to the initiation of the system's motion. At the end of the movement, a significant increase in force can be observed on the graph. This is caused by the sudden stop of the leg, which is associated with modelling the upper stop of the landing gear movement as an almost rigid element. In reality, the deceleration of the landing gear would be much smoother, as rubber bumpers were used in the design.

- **Case 3. Landing gear extension,  $F=3100\text{N}$ ,  $n=2.245$**

Force in the joint for max actuator force, LG extension,  $n=2.245$

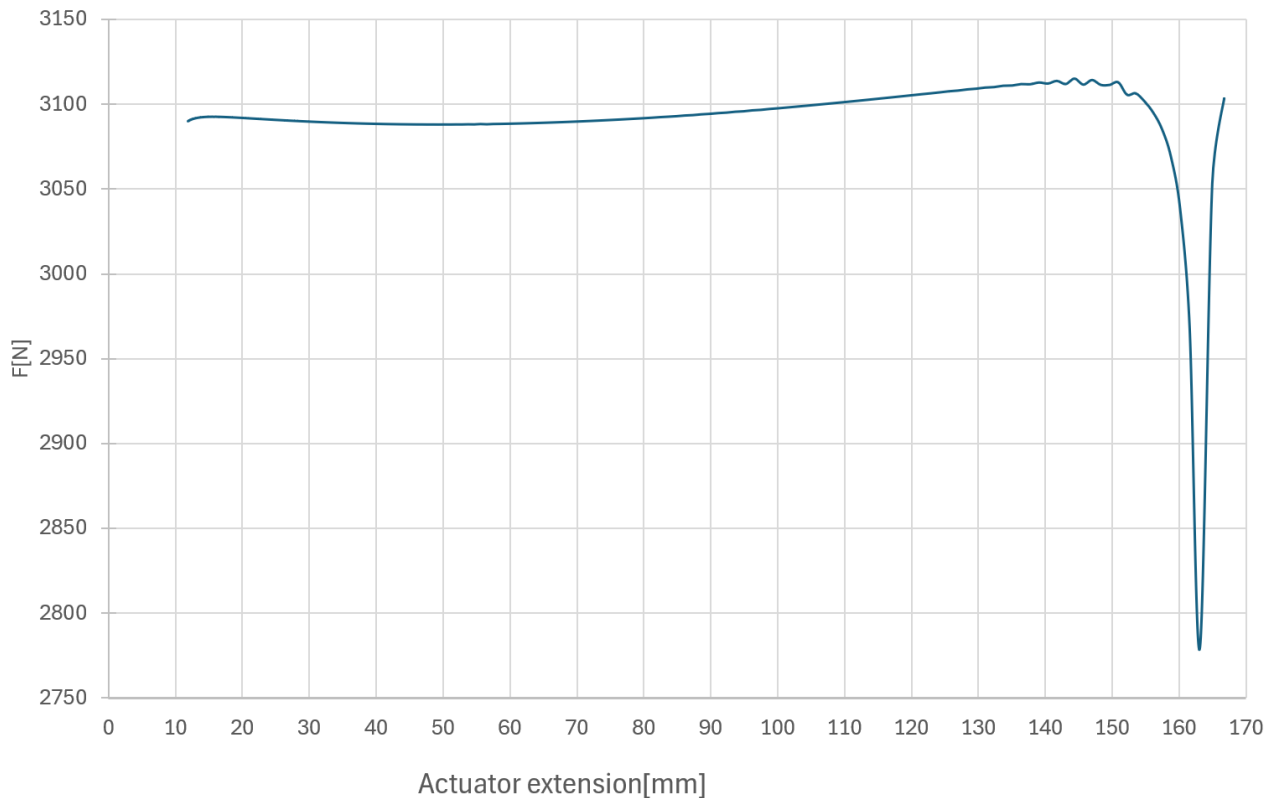


Figure 10 - Force in the actuator joint for max actuator force

The value of the resultant force, as expected, is also nearly constant. There are slight changes associated with the movement of the mass of the entire system. The disturbances occurring for the actuator extension range of 140–155 mm are related to a slightly too long analysis step. At the end of the movement range, there is also a sudden increase in force, the cause of which was already explained in case 1.

- **Case 4. Landing gear retracted, and locked,  $n=5.131$**

A static analysis of the system in the retracted and locked state was conducted. This allowed for the determination of the force acting on the actuator due to the occurrence of vertical acceleration  $n = 5.131$ . The value of the resultant force at the connection of the actuator with the lever in this configuration is:  $F_{max} = 5133.282\text{ N}$ .

- **Case 5. Emergency extension**

A simulation of the emergency landing gear release system was performed. To this end, the rotary pin locking the latch was unlocked, and a force of  $F = 1000\text{ N}$  acting along the axis of the gas spring was applied. The landing gear was extended and locked.

The force is presented as a function of time, as the actuator is locked in one position. The value of the force at the connection changes because, with the rotational movement of the latch, the direction of its application changes. A short moment before the strut locks, there is a sudden increase in force due to the assumed very high stiffness of the system components (analogous to previous cases). Ultimately, the force locking the system is  $F = 670\text{ N}$ .

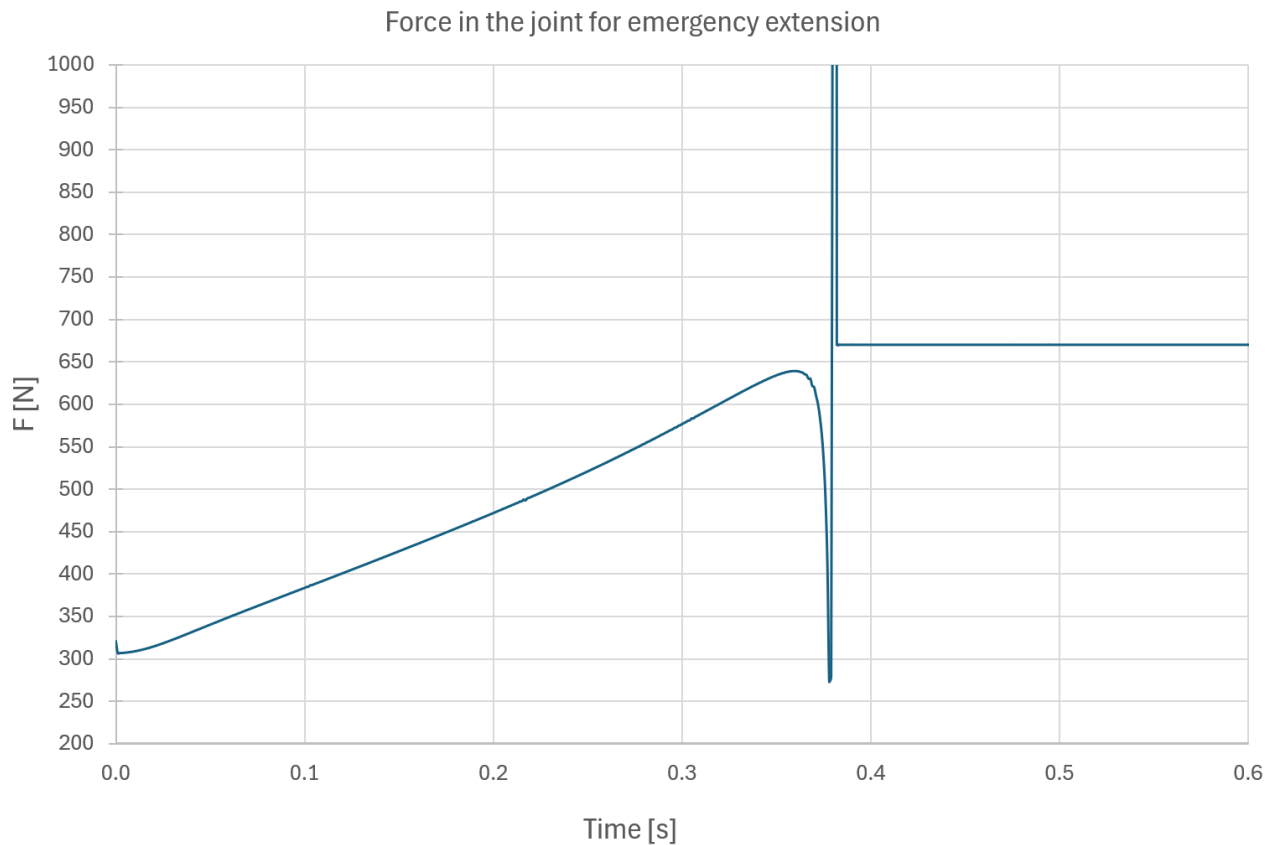


*Figure 11 Force in the joint during emergency extension*

The force is presented as a function of time, as the actuator is locked in one position. The value of the force at the connection changes because, with the rotational movement of the latch, the direction of its application changes. A short moment before the strut locks, there is a sudden increase in force due to the assumed very high stiffness of the system components (analogous to previous cases). Ultimately, the force locking the system is  $F= 670 \text{ N}$

### 3.5 Structural analysis

A necessary stage in the design process is the strength analysis of the modified elements, which determines whether the created components are capable of bearing the required loads.

To determine the strength of the new lever, a computational model using the Finite Element Method was prepared in NX Nastran. The obtained results allowed for the implementation of changes that contributed to reducing the mass of the component.

The lever was modelled using three-dimensional tetrahedral elements as shown in Figure 12. Appropriate material properties for steel 40HM were assigned. The shaft part of the rotating axis was also modelled using three-dimensional tetrahedral elements, with the material used for the shaft being steel 30HGSA. The pins connecting the components were modelled using beam elements with material properties appropriate for steel 40HM.

**KINEMATIC SIMULATION IN THE AIRCRAFT LANDING GEAR DESIGN AND OPTIMIZATION PROCESS**

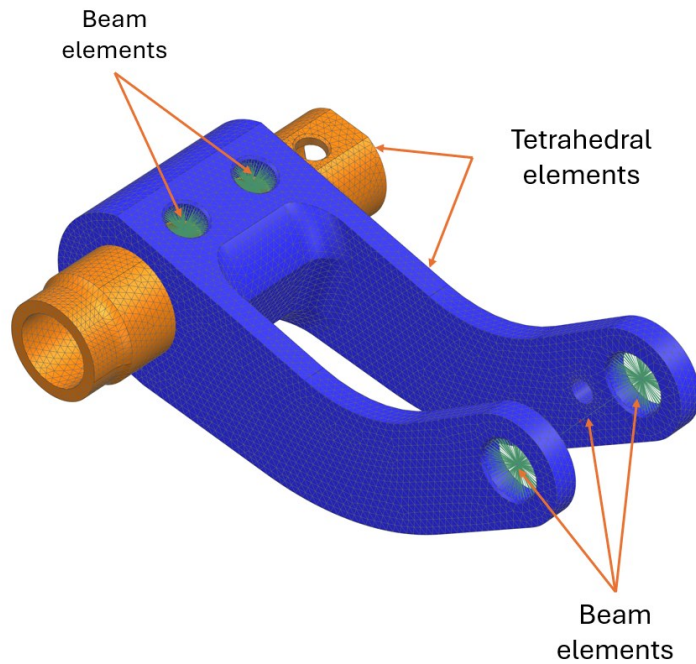


*Figure 12 - FEM model of the lever*

To facilitate the identification of the force components applied to the system, an auxiliary coordinate system was created. Its origin is located at the midpoint between the centres of the holes for the pin. The X-axis is parallel to the normal vector of the surface marked in orange in Figure 13. The Z-axis is defined by the centres of the holes for the pin.

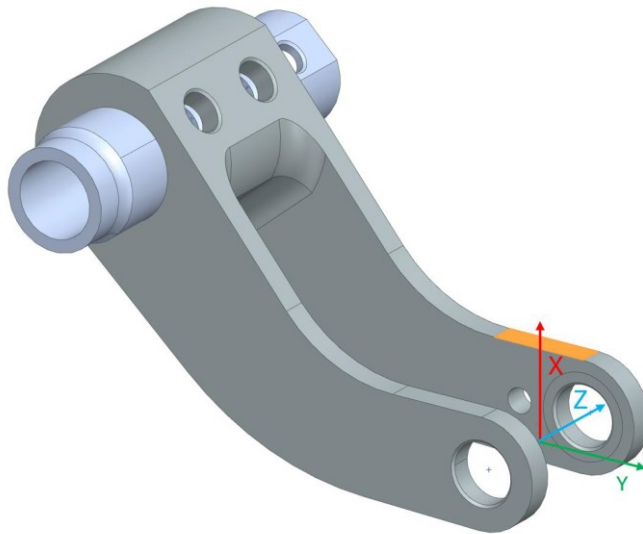


*Figure 13 The lever with a new coordinate system*

There were the analysis for 5 load cases conducted. Additional correction factor  $k=1.1$  was assumed.

- **Case 1. Landing gear retracted,  $n=5.131$**

*Table 2 - Loads for Case 1.*

Case 1. Landing gear retracted $n = 5.131$ ,		
$F_x$	$F_y$	$F_z$
-5626.5N	-440N	0

- **Case 2. Landing gear retracted,  $n=5.131$ , lateral force**

Due to the possibility of slight axial movement of the rotating shaft, there may be situations where the actuator is not perpendicular to the axis of the pin, resulting in the occurrence of a lateral force ( $F_z$ ).

It is therefore assumed that the maximum angle of deviation that may occur in the system is  $\alpha = 5^\circ$ .

Table 3 - Loads for Case 2.

Case 2. Landing gear retracted, $n = 5.131 + lateral\ force$		
$F_x$	$F_y$	$F_z$
-5604.87N	-441.111N	491.876N

- **Case 3. Max force  $F_x$  with lateral force**

In this case, all analyses performed in NX Motion were taken into account, from which the scenario where the force  $F_x$  reached its maximum value was selected. This was the case of extending the landing gear with a force of  $F=3100N$ . For this load, the force distribution was determined when the actuator was deflected by an angle  $\alpha$ .

Table 4 - Loads for Case 3.

Case 3. Max force $F_x$ with max angle deviation		
$F_x$	$F_y$	$F_z$
3080.23N	0N	269.486N

- **Case 4. Max force  $F_y$  with lateral force**

For this computational case, the scenario was selected from all NX Motion analyses where the force  $F_y$  reached its maximum value. This occurred during the retraction of the landing gear with a force of  $F = 3100N$ . For this load, the force distribution was determined when the actuator was deflected by an angle  $\alpha$ .

Table 5 - Loads for Case 4.

Case 4. Max force $F_y$ with max angle deviation		
$F_x$	$F_y$	$F_z$
0N	3075.16N	269.042N

- **Case 5. Minimal force  $F_y$  with lateral force**

In this case, all analyses performed in NX Motion were taken into account, from which the scenario where the force  $F_y$  reached its minimum value was selected. This was the case of extending the landing gear with a force of  $F = 3100N$ . For this load, the force distribution was determined when the actuator was deflected by an angle  $\alpha$ .

Table 6 - Loads for Case 5.

Case 5. Minimal force $F_y$ with max angle deviation		
$F_x$	$F_y$	$F_z$
0N	-3096.09N	270.872N

The stress distributions obtained from the preliminary analyses allowed to conclude that the created computational model accurately represents the real system.

The highest value of the von Mises stress was obtained for case no. 2  $\sigma_{red} = 410.02MPa$

The visualization of stresses in the element is shown in Figure 14.

UKI\_dzwigni\_do\_mesu\_sim1 : Test Result  
Schowane+boczna, Static Step 1  
Stress - Elemental, Averaged, Von-Mises  
Min : 0.33, Max : 1433.38, Units = MPa  
Deformation : Displacement - Nodal Magnitude

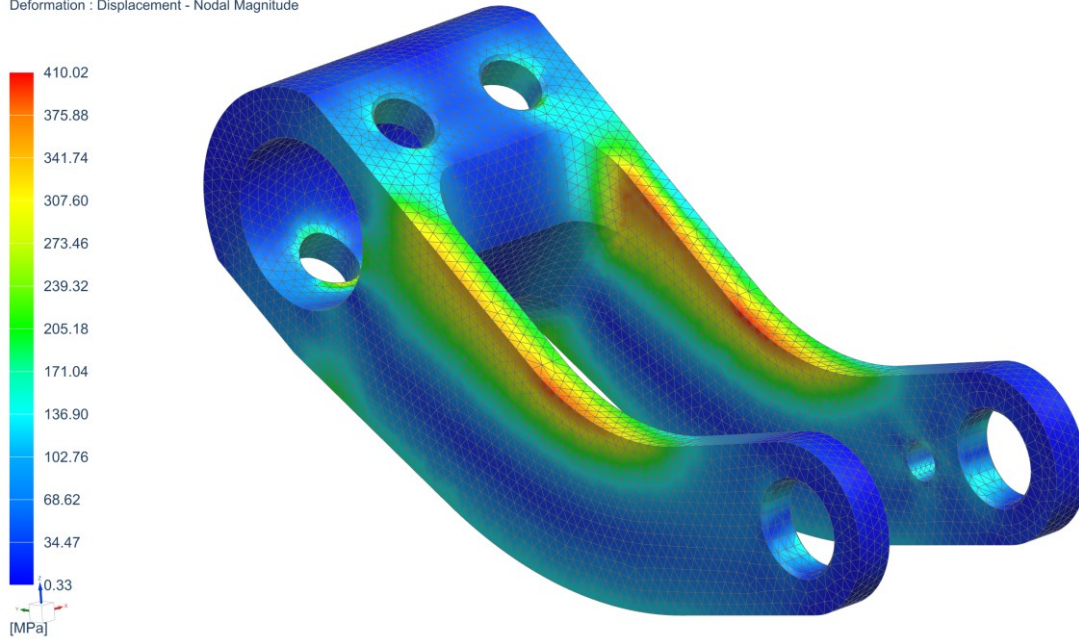


Figure 14 - Stress distribution in the lever for case no. 2

Based on the results of the FEM analysis of the lever, modifications were made that allowed for a reduction in its mass while maintaining appropriate safety margins and the functionality of the system.

The visualization of the lever after implementing the changes is shown in Figure 15.

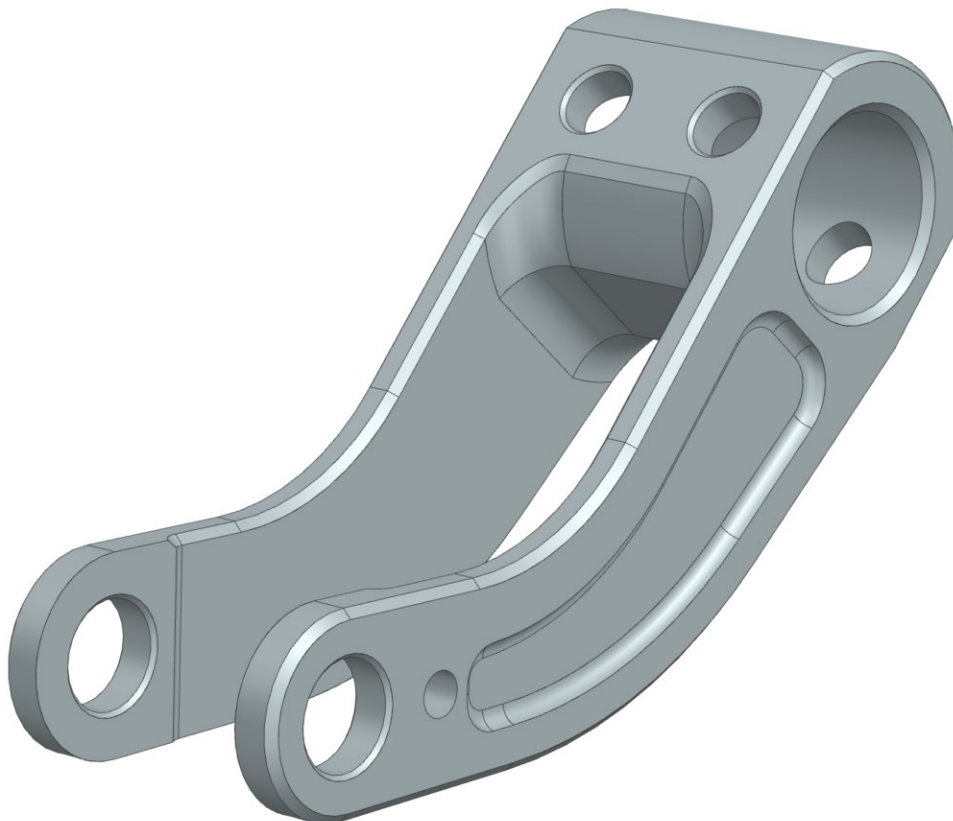


Figure 15 Lever after implementing the changes



The second iteration of the FEM analysis was performed. For case no. 2 stress distribution was shown in Figure 16.

Ukl\_dzwigni\_do\_mesu\_sim1 : Test Result  
 Schowane+boczna, Static Step 1  
 Stress - Elemental, Averaged, Von-Mises  
 Min : 0.27, Max : 1433.52, Units = MPa  
 Deformation : Displacement - Nodal Magnitude

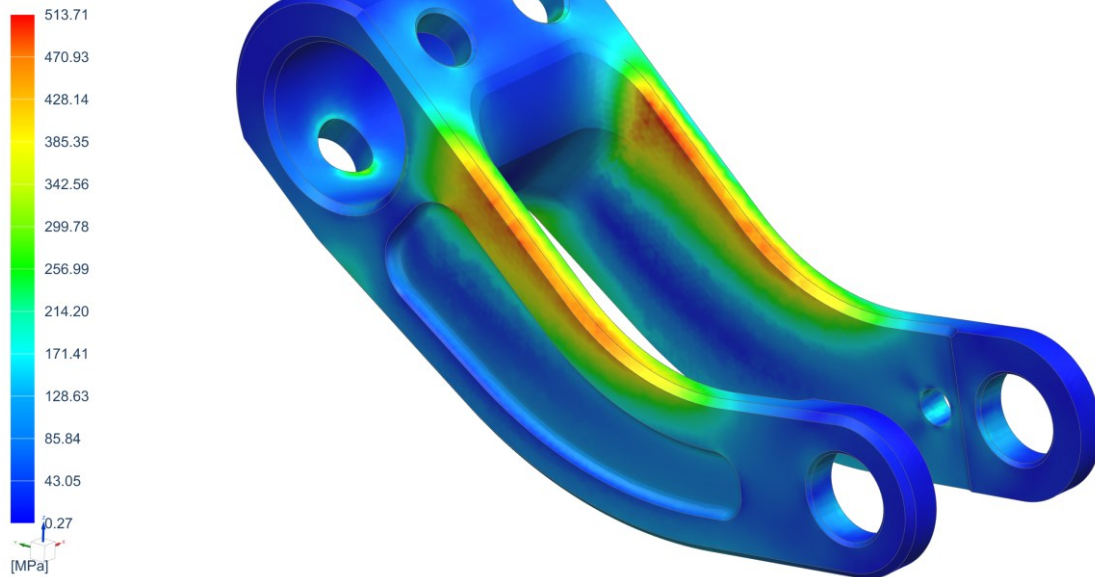


Figure 16 Stress distribution in the lever for case no.2

As a result of the changes in the lever, its mass was reduced, and a uniform stress distribution was achieved, as there are no significant stress concentrations. Max von Mises stress for case no.2 was  $\sigma_{red} = 513.71MPa$ , which corresponds to safety factor of  $x = 1.752$ . The modifications can be safely implemented into the system and will not have a negative impact on the functionality.

#### 4. Conclusion

The article explores the use of CAD (Computer-Aided Design) and CAE (Computer-Aided Engineering) systems in the redesign and analysis of an aircraft landing gear deployment system. The modifications began with the selection of a new actuator to improve system performance and reliability. Following this, a new lever was designed to work with the updated actuator. The design process leveraged advanced CAD tools to create detailed models of the system components, ensuring precision in the geometry and functionality of the new parts.

After the initial design phase, kinematic studies were performed to analyse the movement and behaviour of the updated landing gear system. These analyses focused on how the new components, particularly the actuator and lever, interacted during the extension and retraction of the landing gear. The kinematic study provided critical insights into the dynamics of the system, ensuring that it operated smoothly and within the expected parameters.

Based on the results of the kinematic analysis, the next step involved strength testing of the newly designed lever using CAE tools, specifically the Finite Element Method (FEM). These tests were essential for evaluating the structural integrity of the lever under operational loads and stress conditions. The strength analysis confirmed that the new lever could withstand the required forces without compromising safety or performance, and adjustments were made to ensure an optimal balance between weight reduction and mechanical strength.

The integration of CAD/CAM/CAE technologies throughout the design, analysis, and testing stages allowed for a streamlined workflow that improved accuracy and efficiency. These systems enabled to optimize the landing gear system, ensuring that the redesigned components met both functional and safety standards, while also achieving a reduction in weight and improved overall system performance..

## 5. Contact Author Email Address

[Jakub.suszynski.stud@pw.edu.pl](mailto:Jakub.suszynski.stud@pw.edu.pl)

[Mariusz.kowalski@pw.edu.pl](mailto:Mariusz.kowalski@pw.edu.pl)

[Tomasz.antoniewski@atp-aviation.com](mailto:Tomasz.antoniewski@atp-aviation.com)

## 6. Copyright Statement

The authors confirm that they, and/or their company or organization, hold copyright on all of the original material included in this paper. The authors also confirm that they have obtained permission, from the copyright holder of any third party material included in this paper, to publish it as part of their paper. The authors confirm that they give permission, or have obtained permission from the copyright holder of this paper, for the publication and distribution of this paper as part of the READ proceedings or as individual off-prints from the proceedings.

## References

- [1] Kachel S, Łącki T, Jarzębiński L, Borcuch D. Problemy badań wytrzymałościowych podwozi samolotów lekkich. *Przegląd Mechaniczny*. 2017;6:33–35.
- [2] Abraszek P., *ATP-Aviation Sp.z.o.o.*, Mielec, 2024.
- [3] European Aviation Safety Agency, "Certification Specifications, Acceptable Means of Compliance and Guidance Material for Sailplanes and Powered Sailplanes (CS-22)", Amendment 3, Annex to ED Decision 2021/013/R, 15.09.2021
- [4] Gronowicz Antoni, „Podstawy analizy układów kinematycznych”, Oficyna Wydawnicza Politechniki Wrocławskiej, Wrocław 2003, ISBN 83-7085-672-1
- [5] Dobrzański Tadeusz, „Rysunek Techniczny Maszynowy”, Wydawnictwa Naukowo-Techniczne, Warszawa 2004, ISBN 83-204-3029-1
- [6] Siemens, NX Motion Documentation, <https://docs.sw.siemens.com/pl-PL/documents/209349590/PL20190701150722612>, access: 10.10.2024